Rare Metal Materials and Engineering
Volume 51, Issue 4, April 2022
Available online at www.rmme.ac.cn

Science Press

Cite this article as: Lv Zhao, Yao Junping, Tang Jinqi, et al. First-Principles Study on Effect of Alloying Elements on 3C-SiC/Mg Interface[J]. Rare Metal Materials and Engineering, 2022, 51(04): 1203-1210.

ARTICLE

First-Principles Study on Effect of Alloying Elements on 3C-SiC/Mg Interface

Lv Zhao, Yao Junping, Tang Jinqi, Chen Zhijun

School of Aeronautical Manufacture Engineering, Nanchang Hangkong University, Nanchang 330063, China

Abstract: Effects of doping single Al, Zn, Cu, Ni, Li, and Zr atoms on interfacial bonding in the 3C-SiC/Mg system were studied using the first-principles method based on density functional theory. The Mulliken charge, overlapping population and density of states of representative Zn and Zr atoms were calculated and analyzed. Results show that the most stable stacking structure of the 3C-SiC/Mg interface model is that 5-layer Mg(0001) is stacked on the 10-layer 3C-SiC(111) surface. Among the six 3C-SiC/Mg model structures, the C-terminated center site model has the largest separation energy, the smallest interfacial spacing and the best interfacial wettability. After doping with Zn atom, Zn and Mg atoms are in the anti-bonding state, resulting in the decrease of the separation work of the 3C-SiC/Mg-Zn system. The decrease of the pseudo-energy gap in the density of states weakens the covalent bond in the 3C-SiC/Mg-Zn system, and this is not conducive to interfacial bonding in the 3C-SiC/Mg-Zn system. After doping with Al, Cu, Ni, Li, and Zr atoms, the separation work of the system increases, and Zr has the best effect on improving the interfacial wettability. After doping with Zr, the anti-bonding state of Mg and Si atoms disappears, and a strong Zr-C covalent bond is formed at the interface between the Zr atom and C atom. The delocalization of the density of states increases, and the bonding ability is enhanced, resulting in a maximum increase in the separation work of the 3C-SiC/Mg-Zr system.

Key words: interface; composite materials; electronic structure; first-principles

Magnesium-based composites are new high-tech industrial materials that are developed and widely used in aerospace, electronics and automobile fields[1-7]. The key problems for the magnesium matrix composites are that the chemical properties of Mg are active and how to control interfacial reaction in the expected direction. Therefore, it is greatly significant to study the influence of the interface on the properties of composite materials[8-10].

The interface is a small area between the matrix and the reinforcement element, which can transfer load and prevent crack expansion. Therefore, how the interface is combined and how well it is bounded directly affect the performance of the composite material[11,12]. The types of composite interface bonding are mainly mechanical, physical, and chemical bonding. Experimental research is difficult to carry out at the atomic scale, but with the rapid development of computer technology, computer simulations have gradually become an important way to conduct studies at the atomic scale. First-principles calculations based on density functional theory rely on building a model by computer and then studying the interface of the composite material at the atomic level to reveal the mechanism of interfacial bonding. Scholars have done a lot of research on interfaces using first-principles tool[13-15]. Liu[16] established six Al(111)/3C-SiC(111) interfacial models, and studied two interfaces doped with Mg atoms using first-principles calculations. The results show that the adhesion work of the top site is the largest when the interface is Si-terminated and C-terminated, and there is mutual diffusion of atoms at the interface. The doping of Mg atoms improves the bonding strength of the Si-terminated interface, but it has almost no effect on the C-terminated interface. The interfacial bonding of the Al(111)/3C-SiC(111) interface is a mixture of covalent, ionic and metallic bonding. Mg doping significantly improves the covalent bonding strength of Si-Al and C-Al bonds. Liu[17] studied the electronic structure, adhesion work, bonding properties, and interfacial energy of

---

Received date: April 30, 2021
Foundation item: National Natural Science Foundation of China (52065046, 51661024)

Corresponding author: Yao Junping, Ph. D., Professor, School of Aeronautical Manufacture Engineering, Nanchang Hangkong University, Nanchang 330063, P. R. China,Tel: 0086-791-83863028, E-mail: 10019@nchu.edu.cn

the Mg(0001)/TiB_2(0001) model. When Mg atoms are combined with the Ti-terminated TiB_2 surface and the B-terminated TiB_2 surface, metal/covalent mixed bonds and ionic bonds form, respectively. The interfacial energy of the Mg/TiB_2 interface is much higher than that of the α-Mg/Mg melt interface, and this indicates that the nucleation ability of TiB_2 particles to α-Mg grains is poor from a thermodynamic point of view. Wu[18] studied the interfacial bonding of Al(111)/6H-SiC(0001) and the fracture characteristics of the interface when it is stretched along the *z*-axis. The adhesion work of the C-terminated interface of Al(111)/6H-SiC(0001) is 2.689 J/m^2, which is higher than that of the Si-terminated interface (1.649 J/m^2). The C-terminated interface has a higher tensile strength than the Si-terminated interface. The strength of the two composite materials is higher than that of pure aluminum, but the ductility is weaker. Wang[19] calculated the atomic structure, ideal adhesion work, and electronic structure of the Al/TiC interface, and they found that the ideal adhesion work of the C-terminated Al(121)/TiC(111) interface is much greater than that of the Ti-terminated Al(121)/TiC(111) interface. The interfacial bonding is mainly Al-C ionic and covalent bonding and Al-Ti metallic bonding, and Al-C ionic and covalent bonds are much stronger than Al-Ti metallic bonds .

Many scholars used first-principles calculation to study the interface of composite materials. SiC/Mg composite materials are currently one of the most widely used composite materials. Research regarding SiC/Mg composites is mainly at the macroscopic level. Research on first-principles calculation of the interface in SiC/Mg composites is rare, especially the doping of alloy elements at the interface of SiC/Mg composites. Therefore, the effects of doping alloying elements (Al, Zn, Cu, Ni, Li, Zr) in the Mg matrix on the interface of SiC/Mg composites were studied by first-principles calculations.

1 Calculation and Model Building

1.1 Calculation method

The method used in this study is based on the first-principles density functional theory calculations[20-23]. One of the modules in Materials Studio-Castep was used[24,25]. A plane-wave ultra-soft pseudo-potential was used to describe the interaction between electrons and ions. Self-consistent field (SCF) and the Broyden-Fletcher-Goldfarb-Shannon (BFGS) algorithm were used for energy calculations. For geometric optimizations, the energy convergence accuracy was 1.0×10^{-5} eV/atom, the maximum force on each atom was 0.3 eV/nm, the maximum stress should not be greater than 0.05 GPa, and the displacement deviation was less than 0.0001 nm.

The unit cell models of 3C-SiC and Mg can be directly imported from the structure model library in Materials Studio. 3C-SiC has a zinc blende structure (cubic phase), the space group is F-43m, and there are 4 Si atoms and 4 C atoms in the primitive cell. The lattice parameter is *a*=0.4348 nm. Mg belongs to a close-packed hexagonal structure, the space point group is P63/MMC, and the space group number is 194. The primitive cell is composed of two Mg atoms, and the lattice constants are *a*=0.320 94 nm, *c*=0.521 05 nm.

1.2 Calculation parameters

1.2.1 Potential function

Suitable exchange correlation potential functions (such as LDA, GGA-PBE, GGA-RPBE, and GGA-PW91) are different for different material simulation systems[26,27]. Therefore, a potential function selection test of the studied 3C-SiC/Mg interface system should be carried out to determine the most suitable functional type. Different exchange correlation potential functions were selected to calculate the structural optimization of the 3C-SiC block and Mg block. The theoretical lattice parameters after structural optimization were compared with previous experimental values to determine the deviation values. The functional with the minimum deviation value was selected for further research and calculation of the volume phase and interface. Table 1 shows the geometric optimization results for the Mg unit cell, and Table 2 shows the geometric optimization results for the 3C-SiC unit cell. From these comparisons, it is determined that GGA-PBE is the best functional for the system studied in this research.

1.2.2 Cut-off energy

Selecting the cut-off energy is an important step in calculating the parameters of the CASTEP module. The level of the cut-off energy is closely related to the number of plane waves. If the cut-off energy is set too low, the calculation accuracy of the system will be affected. If the cut-off energy is set too high, the calculation accuracy will be improved, and the calculation amount also increases with an increase in the number of plane waves. Therefore, the choice of cut-off energy for different calculation systems becomes particularly important. In this research, GGA-PBE was selected as the

Table 1 Geometric optimization results for Mg

Method	$a/\times10^{-1}$ nm	$c/\times10^{-1}$ nm	Error of a/%	Error of c/%
LDA	3.159 659	5.076 627	−1.550	−2.569
GGA-PBE	3.222 132	5.170 649	0.397	−0.765
GGA-RPBE	3.250 088	5.215 844	1.268	0.103
GGA-PW91	3.225 257	5.175 315	0.494	−0.675
GGA-WC	3.210 306	5.157 616	0.028	−1.015
GGA-PBESOL	3.204 988	5.149 941	−0.137	−1.162

Table 2 Geometric optimization results for 3C-SiC

Method	$a/\times10^{-1}$ nm	Error of a/%
LDA	4.304 029	−1.236 2
GGA-PBE	4.366 527	0.198 0
GGA-RPBE	4.372 254	0.329 4
GGA-PW91	4.367 863	0.228 6
GGA-WC	4.363 835	0.136 2
GGA-PBESOL	4.365 864	0.182 7

exchange correlation potential functional. Other parameters were fixed, and the calculation precision was fine. The range of the tested cut-off energy was 220~500 eV. The energy values obtained for the 3C-SiC unit cell and Mg unit cell under different truncation energies were analyzed by gradually increasing the cut-off energy. The influences of the cut-off energy on the stability of the energy calculation accuracy for the Mg and 3C-SiC systems are shown in Fig.1. When the cut-off energy was greater than 380 eV, the energy of the 3C-SiC and Mg systems tends to be stable, and further increasing the cut-off energy has little impact on the stability of the system. Therefore, in this research, the cut-off energy was set to 380 eV.

1.2.3 K-point

The size of the K-point is related to the precision of the electron density of the calculation system. When the choice of K-point is greater, the precision of calculation is higher, and the amount of calculation is larger. Other parameters were kept constant. For the fine calculation accuracy, the cut-off energy was selected to be 380 eV, the value of K-point increased, and the convergence relationship between the K-point and total energy was calculated and analyzed. The influence of the K-point on the stability of the total energy of Mg and 3C-SiC is shown in Fig.2. When the K-point is 6, the energy begins to converge. Comprehensively, the K-point used in the calculation of the bulk properties was selected as 6×6×6, the K-point used in the calculation of the surface properties and interface properties was selected as 6×6×1 in this research.

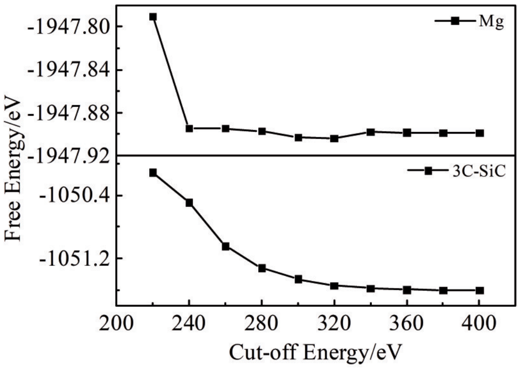

Fig.1 Influences of the cut-off energy on the stability of energy calculation accuracy for Mg and 3C-SiC

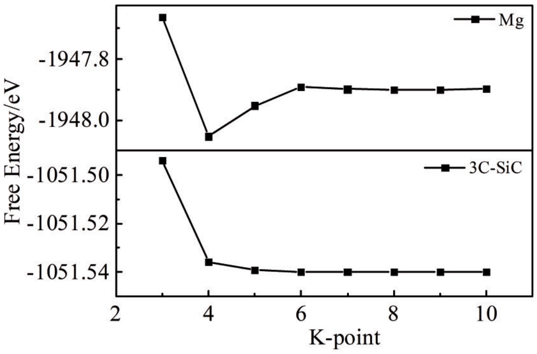

Fig.2 Influences of the K-point on the stability of the total energy of Mg and 3C-SiC

1.3 Calculation model

1.3.1 Mg and 3C-SiC bulk properties

Fig.3 shows the density of states and energy band structure of the Mg bulk phase. As seen Fig.3a, there are multiple main peaks for bonding states between −6.5~14 eV. The high density of states at the Fermi level indicates that the Mg electrons are strongly delocalized and show strong conductivity. As seen in Fig. 3b, the valence band and conduction band overlap, and the energy gap is 0, indicating strong metallicity. The electrons can easily gain energy and jump to the upper conduction band to conduct electricity.

Fig.4 shows the density of states and energy band structure of the 3C-SiC bulk phase. As shown in Fig.4a, the density of states of the 3C-SiC bulk phase is divided into three parts, which are −15.5~−9.6 eV , −8.2~0.4 eV and 1.6~16.8 eV. The first part is mainly controlled by C-2s; in the second part, C-2p has the main role; in the third part, C-2p and Si-3p have strong hybridization. Because of the p-p orbital hybridization, a strong covalent bonding forms. The value of the density of states at the Fermi level is not 0, indicating that the 3C-SiC bulk phase has weak metallicity. Because 3C-SiC is a semiconductor material, the energy gap between the valence band and conduction band is small (1.4 eV), as seen in the energy band structure of Fig.4b.

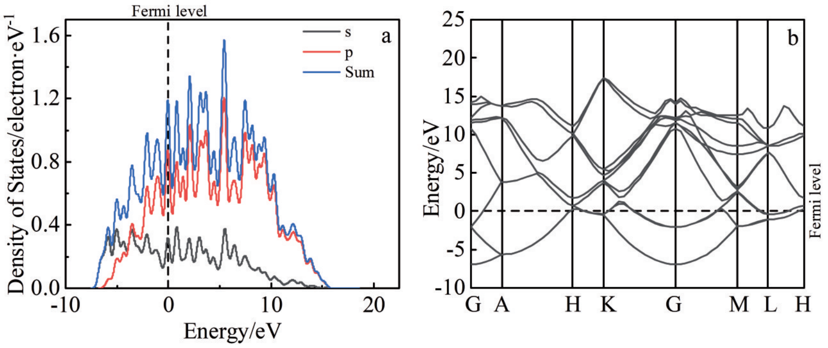

Fig.3 Density of states (a) and energy band structure (b) of Mg bulk phase

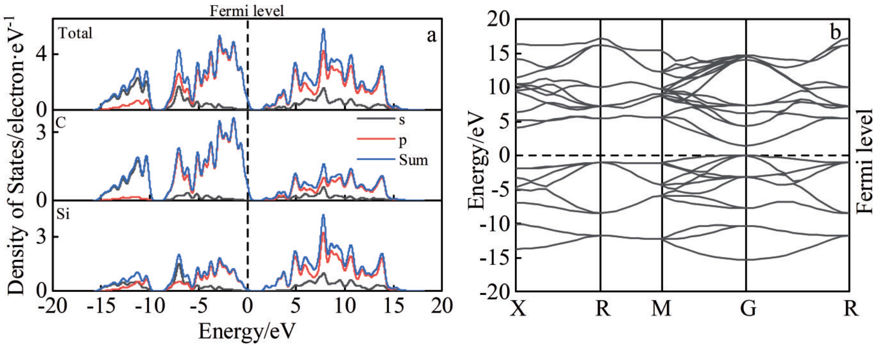

Fig.4 Density of states (a) and energy band structure (b) of 3C-SiC bulk phase

1.3.2 Surface energy and stability of Mg and 3C-SiC

When the two crystal phases are combined, the surface with low surface energy is usually selected for combination. Therefore, it is necessary to calculate and analyze the structure and total energy of several common planes of Mg, and to establish representative surface structure models of Mg crystal, such as Mg(0001), Mg($10\bar{1}0$), Mg($10 1\bar{1}$) and Mg ($11\bar{2}2$), as shown in Fig.5.

Formula for calculating the surface energy is

$$E_{\text{surf}}=\frac{E_{\text{slab}}-(\frac{N_{\text{slab}}}{N_{\text{bulk}}})E_{\text{bulk}}}{2A} \tag{1}$$

where E_{surf} is the total energy of the system with a vacuum layer added after section, N is the number of atoms, E_{bulk} is the energy of the primitive cell, and A is the surface area of the surface model.

The calculation results for the surface energy of common planes of Mg are shown in Table 3. The order of the surface energy of common planes of Mg is Mg(0001)<Mg($10\bar{1}0$)<Mg($101\bar{1}$)<Mg($11\bar{2}2$). When constructing the interface, the surface with a low surface energy is preferentially selected as the bonding interface. Because the surface of 3C-SiC(111) and Mg(0001) are diamond-shaped, the mismatch of the interface is very small. Therefore, the Mg(0001) and 3C-SiC(111) are selected as the bonding interface.

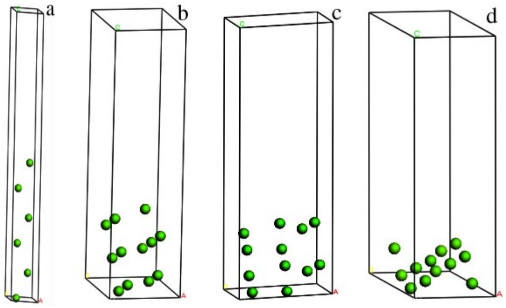

Fig.5 Surface structure models of Mg(0001) (a), Mg($10\bar{1}0$) (b), Mg ($101\bar{1}$) (c) and Mg($11\bar{2}2$) (d)

Table 3 Surface energy of common planes of Mg (J·m^{-2})

Model	Mg(0001)	Mg($10\bar{1}0$)	Mg($10\bar{1}1$)	Mg($11\bar{2}2$)
Surface energy	0.314	0.606	0.617	0.619

Because there is only one kind of atom in the Mg cell structure, the Mg(0001) plane is nonpolar plane. When the number of atomic layers is an even number and the sealed ends are Si and C, the upper and lower surfaces are atoms with an unsaturated bond, and the 3C-SiC(111) plane is a polar plane. With an increase in the number of layers, the energy of the surface model converges. A convergence test was carried out for the Mg(0001) surface model, and the 3C-SiC(111) surface model has a gradually increasing number of atomic layers.

The minimum number of layers of the Mg(0001) surface model can be determined according to the following formula:

$$\Delta E=E_{\text{S}}^{N}-E_{\text{S}}^{N-2} \tag{2}$$

ΔE is the total energy difference of the surface model, E_{S}^{N} is the total energy of the surface model with N layers after structural optimization, and E_{S}^{N-2} is the total energy of the surface model with N−2 layers after structural optimization. When the number of layers n reaches a certain critical value N, the total energy difference of the surface model will tend to a value reaching the condition of convergence. When the value of n is greater than N, the total energy difference of the Mg(0001) surface is stable at a numerical value, and does not change greatly.

The calculation results for the surface energy of Mg(0001) are shown in Table 4. As seen from it, when the number of layers is greater than 3, the total energy difference of the surface model is −1947.97 eV. It is only necessary to keep the internal structure of the Mg(0001) surface model the same to prevent an increase in the size of the calculation. Therefore, the Mg(0001) part of the interface model has a 5-layer structure.

The calculation results for the surface energy of 4~14 layers of 3C-SiC(111) are shown in Table 5. As seen from it,

Table 4 Surface energy of Mg(0001) (eV)

Layers (N-2)	3~5	5~7	7~9	9~11	11~13
ΔE	−1947.973 6	−1948.010 2	−1947.967 9	−1947.977 1	−1947.960 5

Table 5 Surface energy of 3C-SiC(111) ($J\cdot m^{-2}$)

Layer number	4	6	8	10	12	14
Surface energy	1.88	3.39	3.72	3.77	3.77	3.77

when the number of atomic layers is 10, the surface energy starts to converge to 3.77 J/m^2. Therefore, the number of atomic layers of the 3C-SiC(111) plane was selected as 10 layers.

1.3.3 Separation work and interfacial stability of 3C-SiC/Mg

According to the above convergence test results for surface energy, the 3C-SiC/Mg interface model was constructed as follows: the 5-layer Mg(0001) surface was built on the 10-layer 3C-SiC(111) surface, and the thickness of the vacuum layer was selected as 1.5 nm. Considering that the 3C-SiC (111) surface has two types of Si terminals and C terminals, and there are three stacking methods of interface model: hollow site, center site and top site, a total of 6 interface models are constructed, as shown in Fig.6.

The bonding strength of an interface is usually measured in terms of the separation work, which is the energy required to separate an interface into two free surfaces. The formula to calculate separation work is as follows:

$$W_{\mathrm{sep}}=\frac{E_{\mathrm{SiC}}^{\mathrm{slab}}+E_{\mathrm{Mg}}^{\mathrm{slab}}-E_{\mathrm{SiC/Mg}}^{\mathrm{total}}}{A} \tag{3}$$

$E_{\mathrm{SiC}}^{\mathrm{slab}}$ and $E_{\mathrm{Mg}}^{\mathrm{slab}}$ are the energy of the 3C-SiC(111) surface and Mg(0001) surface after structural optimization, respectively, $E_{\mathrm{SiC/Mg}}^{\mathrm{total}}$ is the energy of the 3C-SiC(111)/Mg(0001) interface after structural optimization, and A is the surface area of the 3C-SiC(111)/Mg(0001) interface.

The separation work and interfacial spacing of the 3C-SiC (111)/Mg(0001) interface are shown in Table 6. As seen from the table, different stacking methods have great influences on the interfacial spacing and the separation work of the interface model after structural optimization. For the interface models with different terminals, the maximum separation work of the C-terminated interface is greater than the maximum separation work of the Si-terminated interface, and the minimum interfacial spacing of the C-terminated interface is smaller than the minimum interfacial spacing of the Si-terminated interface. These observation indicates that the C-terminated model is more stable. Among the three stacking methods for the C-terminated interface, the center site model has the largest separation work and the smallest interfacial spacing, and it is the most stable of all of the interface models.

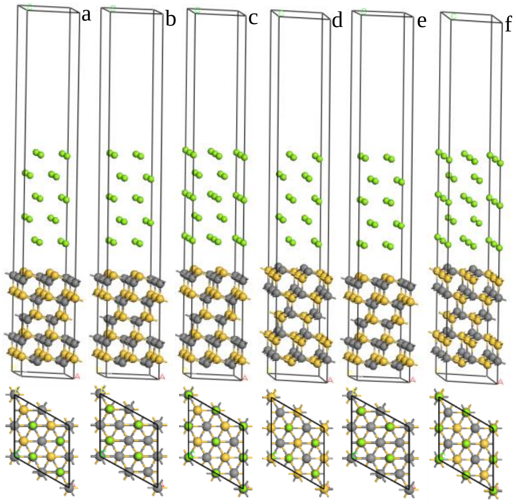

Fig.6 Six interface models of 3C-SiC/Mg interface: (a) Si-terminated center site, (b) Si-terminated top site, (c) Si-terminated hollow site, (d) C-terminated center site, (e) C-terminated top site, and (f) C-terminated hollow site

Table 6 Separation work and interfacial spacing of the 3C-SiC (111)/Mg(0001) interface

Termination	Stacking	W_{sep}/ $J\cdot m^{-2}$	Unrelaxed, $d_o/\times10^{-1}$ nm	Fully relaxed $d_o/\times10^{-1}$ nm
Si-terminated	Center	1.8053	3.83	2.3024
	Top	1.7155	3.83	2.7086
	Hollow	1.6519	3.83	2.9071
C-terminated	Center	2.5834	3.43	1.7193
	Top	2.4104	3.43	2.1950
	Hollow	2.2477	3.43	2.3318

Al, Zn, Cu, Ni, Li, and Zr are common elements in magnesium alloys. Changing material properties via doping has been a hot topic in experimental and theoretical research. According to the theory of interfacial adsorption driven wetting proposed by Saiz[28], alloying elements are preferentially concentrated at the interface. On the basis of the results of the above structural optimizations, a model of the C-terminated center site structure of the 3C-SiC(111)/Mg(0001) interface was constructed. Using this interface model, a 3C-SiC/Mg-X(X=Al, Zn, Cu, Ni, Li, Zr) interface structure model doped with 6 elements was established. Because the system is unstable after doping with atoms, it is necessary to optimize the structural model after doping, so that the atoms in the whole system are fully relaxed and reach a stable state. Fig.7 shows the 3C-SiC/Mg model before doping and the 3C-SiC/Mg-X model after doping.

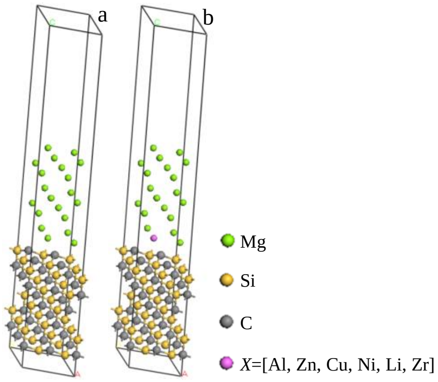

Fig.7 3C-SiC/Mg model before doping (a) and 3C-SiC/Mg-X model after doping (b)

2 Results and Discussion

2.1 Influence of doping atoms on the interfacial separation work

Data for the separation work of 3C-SiC/Mg before doping and the 3C-SiC/Mg-*X* system after doping are shown in Table 7. The greater the separation work, the better the wettability of the interface, and the greater the bonding strength of the interface. As seen from the table, when Zn, Cu, Ni, and Zr atoms replace one Mg atom at the interface, the total energy of the system becomes larger, and this is because of different degrees of distortion of the structure after atoms are replaced. The total energy of the system becomes smaller after the Mg atom was replaced with Al and Li atoms. Doping with a Zn atom results in a significant decrease in the separation work, and this indicates that Zn has a negative effect on the interfacial bonding of the 3C-SiC/Mg-Zn system. After doping with other atoms (Al, Cu, Ni, Li, and Zr), the separation work of the interface increased to different degrees: 2.639, 2.869, 3.014, 3.002, and 3.225 J/m^2, respectively. Among them, the separation work increased by Al doping is the least, and doping with Zr has the most significant effect on the interfacial bonding of the 3C-SiC/Mg-Zr system.

2.2 Influences of doping atoms on the electronic structure of the interface

To determine the mechanism of the effect of doping alloy elements on the 3C-SiC /Mg interface, the effects of the doped Zn atom with the minimum interface adhesion work and the doped Zr atom with the maximum adhesion work on the electronic structure of 3C-SiC /Mg system are discussed separately. The Mulliken charges of the 3C-SiC/Mg, 3C-SiC/Mg-Zn and 3C-SiC /Mg-Zr systems are shown in Table 8. As seen from it, when the interface is formed, C and Zr atoms mainly have electrons in p orbitals. The Mg atom mainly loses electrons from the p orbital, and the Zn atom mainly loses electrons from the d orbital.

The overlap layout number is used to represent the parameters of interaction between atoms. The size of the value indicates the strength of a bond between atoms. A positive value indicates that there is a covalent bond; a negative value indicates that there is an anti-bond and that the atoms mutually repel each other. The populations of the 3C-SiC/Mg, 3C-SiC/Mg-Zn, and 3C-SiC/Mg-Zr systems are shown in Table 9. After doped Zn, the Zn and Mg atoms repel each other, an anti-bond (−0.33) form, and Zn does not combine with Si and C atoms. After doping with Zr, the Zr atom, a strong covalent bond forms with the C atom on the 3C-SiC side, and the population is 0.50. The anti-bond between Mg and Si atoms disappears, and Zr and Si atoms are in the weak anti-bonding state.

Table 7 Separation work of 3C-SiC/Mg before doping and 3C-SiC/Mg-*X* after doping

Model	Total energy/eV	W_{sep}/J·m^{-2}
3C-SiC/Mg	−24 724.954 17	2.583
3C-SiC/Mg-Al	−23 807.247 89	2.639
3C-SiC/Mg-Zn	−25 459.921 79	2.207
3C-SiC/Mg-Cu	−25 227.583 66	2.869
3C-SiC/Mg-Ni	−25 105.621 34	3.014
3C-SiC/Mg-Li	−23 942.067 66	3.002
3C-SiC/Mg-Zr	−25 032.231 27	3.225

Table 8 Mulliken charges of 3C-SiC/Mg, 3C-SiC/Mg-Zn and 3C-SiC/Mg-Zr

Model	Atom	Charge population				
		s	p	d	Total	Charge
3C-SiC/Mg	Mg	0.67	6.71	0.00	7.38	0.62
	C	1.51	3.77	0.00	5.28	−1.28
3C-SiC/Mg-Zn	Mg	0.67	6.59	0.00	7.26	0.74
	C	1.51	3.74	0.00	5.25	−1.25
	Zn	0.76	1.23	9.99	11.97	0.03
3C-SiC/Mg-Zr	Mg	0.68	6.68	0.00	7.36	0.64
	C	1.48	3.69	0.00	5.18	−1.18
	Zr	2.42	6.78	2.83	12.03	−0.03

Table 9 Populations of 3C-SiC/Mg, 3C-SiC/Mg-Zn and 3C-SiC/Mg-Zr

Model	Bond type	Population
3C-SiC/Mg	C-Mg	−0.05
	Mg-Si	−0.25
3C-SiC/Mg-Zn	C-Mg	−0.12
	Mg-Zn	−0.33
	Mg-Si	−0.26
3C-SiC/Mg-Zr	C-Mg	−0.01
	Zr-C	0.50
	Zr-Si	−0.08

The densities of states of Mg and C atoms in the interface before and after doping with Zn and Zr atoms are shown in Fig.8. The density of states changes significantly after doping with Zn and Zr. After doping with Zn, the wave peaks of the anti-bonded states of Mg and C atoms in the interfacial layer increase below the Fermi level. The pseudo energy gap after doping is significantly smaller than that before doping, and the covalent bond is weaker. After doping with Zr, the peak value of Mg and C atoms at the interface increases at the Fermi levels, indicating that the atoms have stronger metallic properties. The distribution of the density of states becomes wider, the peak value of the density of states decreases, the delocalization increases, and the bonding ability of interfacial atoms is enhanced.

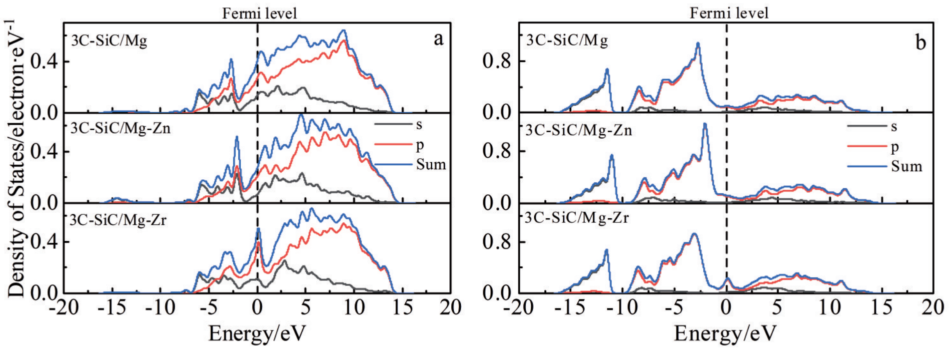

Fig.8 Density of states of Mg (a) and C (b) atoms in the interface before and after doping with Zn and Zr

3 Conclusions

1) When the number of layers on the Mg(0001) surface is greater than 3, the surface energy converges to −1947.97 eV. When the number of layers on the 3C-SiC(111) surface is 10, the surface energy converges to 3.77 J/m^2, and the stacking structure of the 5-layer Mg(0001) surface on the 10-layer 3C-SiC(111) surface is the most stable. The center site model has the largest separation work and the smallest interfacial spacing among the three stacking methods. By this stacking method, the separation work of the C-terminated structure is greater than that of the Si-terminated structure, and the interfacial spacing of the C-terminated structure is smaller than that of the Si-terminated structure. The C-terminated center site structure is the most stable among the six 3C-SiC(111)/Mg (0001) models.

2) When Zn atoms are doped at the interface of the 3C-SiC/Mg system, the separation work decreases. After doping with Zn atom, the Zn and Mg atoms repell each other, and it does not combine with Si and C atoms. Wave peaks of the anti-bonding state increase, the pseudo energy gap decreases, and the covalent bonding of the 3C-SiC/Mg-Zn system is weaker.

3) When Al, Cu, Ni, Li, and Zr atoms are doped at the interface of the 3C-SiC/Mg system, the separation work of system is improved, and the improvement in the separation work after doping with Zr atom is the most significant. After doping with Zr atoms, a strong covalent bond forms between the Zr and C atoms, the peak value at the Fermi level increases, the delocalization is enhanced, and the bonding ability is enhanced.

References

1 Shimizu Y, Miki S, Soga T *et al. Scripta Materialia*[J], 2008, 58(4): 267

2 Li L, Lai M O, Gupta M *et al. Journal of Materials Science*[J], 2000, 35(22): 5553

3 Xu W, Birbilis N, Sha G *et al. Nature Materials*[J], 2015, 14(12): 1229

4 Ye H Z, Liu X Y. *Journal of Materials Science*[J], 2004, 39(20): 6153

5 Abbott T B. *Corrosion* [J], 2015, 71(2): 120

6 Morisada Y, Fujii H, Nagaoka T *et al. Materials Science and Engineering A*[J], 2006, 419(1-2): 344

7 Ding Wenjiang, Fu Penghuai, Peng Liming *et al. Spacecraft Environment Engineering*[J], 2011, 28(2): 103 (in Chinese)

8 Finnis M W. *Journal of Physics: Condensed Matter*[J], 1996, 8(32): 5811

9 Wang S Q, Ye H Q. *Current Opinion in Solid State and Materials Science*[J], 2006, 10(1): 26

10 Zhang C, Yao D, Yin J *et al. Materials Science and Engineering A*[J], 2018, 723: 109

11 He P, Huang S, Wang H *et al. Ceramics International*[J], 2014, 40(10): 16 653

12 Marten T, Alling B, Isaev E I *et al. Physical Review B*[J], 2012, 85(10): 104 106

13 Li C M, Jiang X Q, Chen N P *et al. Rare Metal Materials and Engineering*[J], 2020, 49(8): 2557

14 Zhu L Q, Wang W F, Jiang Y *et al. Rare Metal Materials and Engineering*[J], 2018, 47(10): 3058 (in Chinese)

15 Pang Y, Guan W M, Chen S *et al. Rare Metal Materials and Engineering*[J], 2011, 40(1): 80 (in Chinese)

16 Liu B, Yang J. *Journal of Alloys and Compounds*[J], 2019, 791: 530

17 Liu R, Yin X, Feng K *et al. Computational Materials Science*[J], 2018, 149: 373

18 Wu Q, Xie J, Wang C *et al. Surface Science*[J], 2018, 670: 1

19 Wang Z J, Liu S, Qiu Z X *et al. Applied Surface Science*[J], 2020, 505: 144 502

20 Tao Y, Xue Q, Liu Z *et al. ACS Applied Materials & Interfaces*[J], 2014, 6(11): 8048

21 Wang H L, Tang J J, Zhao Y J *et al. Applied Surface Science*[J], 2015, 355: 1091

22 Xiong H, Liu Z, Zhang H *et al. Journal of Physics and Chemistry of Solids*[J], 2017, 107: 162

23 Sabzyan H, Sadeghpour N. *Zeitschrift für Naturforschung A*[J], 2017, 72(1): 1

24 Clark S J, Segall M D, Pickard C J *et al. Zeitschrift für Kristallographie*[J], 2005, 220(5-6): 567

25 Segall M D, Lindan P J D, Probert M J *et al. Journal of Physics: Condensed Matter*[J], 2002, 14(11): 2717

26 Marlo M, Milman V. *Physical Review B*[J], 2000, 62(4): 2899

27 Perdew J P, Burke K, Ernzerhof M. *Physical Review Letters*[J], 1996, 77(18): 3865

28 Saiz E, Cannon R M, Tomsia A P. *Oil & Gas Science and Technology*[J], 2001, 56(1): 89

第一性原理研究合金元素对3C-SiC/Mg界面的影响

吕　昭，尧军平，唐锦旗，陈致君

(南昌航空大学 航空制造工程学院，江西 南昌 330063)

摘　要：采用基于密度泛函理论的第一性原理方法，研究掺杂单个Al、Zn、Cu、Ni、Li、Zr原子对3C-SiC/Mg体系界面结合的影响，选取代表性的Zn原子和Zr原子进行Mulliken电荷、重叠布居数和态密度计算分析。结果表明，3C-SiC/Mg界面模型最稳定的堆垛结构是将5层的Mg（0001）堆垛在10层的3C-SiC（111）面上，C封端的中心型模型在6种3C-SiC/Mg模型结构中分离功最大，界面间距最小，界面的润湿性最好；掺杂Zn原子后，3C-SiC/Mg-Zn体系的分离功减小，掺杂的Zn原子与Mg原子成反键，态密度中赝能隙变小使得3C-SiC/Mg-Zn体系的共价键性减弱，不利于3C-SiC/Mg-Zn界面结合；掺杂Al、Cu、Ni、Li、Zr原子后，体系的分离功增大，Zr原子对界面润湿性的改善效果最好。掺杂Zr原子后，界面层Mg原子与Si原子的反键消失，与C原子在界面处形成Zr-C强共价键，态密度离域性增强，成键能力增强，导致3C-SiC/Mg-Zr体系的分离功增大最多。

关键词：界面；复合材料；电子结构；第一性原理

作者简介：吕　昭，男，1996年生，硕士，南昌航空大学航空制造工程学院，江西 南昌 330063，电话：0791-83863028，E-mail：daraole96@163.com